Leveraging multispectral and LiDAR UAV to predict individual tree health: a case study of *Viscum album* in Scots pine forests

Ortiz-Ayuso, J. [1*], Sancho-Knapik, D. [2,3], Saz, M.A. [4,5], Hoffrén, R. [6,7], Domingo, D. [1,7,8]

[1] *EiFAB-iuFOR, Campus de Soria, University of Valladolid, E-42004. Soria, Spain, jorge.ortiz@uva.es, dario.domingo@uva.es*

[2] *Agrifood Research and Technology Centre of Aragón (CITA). Avda Montañana 930, 50059 Zaragoza, Spain, dsancho@cita-aragon.es*

[3] *AgriFood Institute of Aragon (IA2) – IA2 (CITA-University of Zaragoza). Zaragoza, Spain*

[4] *Department of Geography and Regional Planning. Environmental Sciences Institute (IUCA). University of Zaragoza. Pedro Cerbuna 12, 50009 Zaragoza, Spain, masaz@unizar.es*

[5] *Environmental Sciences Institute (IUCA). Climate, water, global change, and natural systems group. University of Zaragoza. Zaragoza, Spain.*

[6] *Pyrenean Institute of Ecology, Spanish National Research Council, Avda. Montañana 1005, 50059 Zaragoza, Spain, rhoffren@ipe.csic.es*

[7] *Environmental Sciences Institute (IUCA). GEOFOREST. University of Zaragoza. Zaragoza, Spain.*

[8] *Department of Geography. University of Valladolid. Valladolid, Spain.*

Abstract

The presence of mistletoe in pine stands has expanded in recent decades, currently threating Mediterranean forests. Mistletoe outbreaks can make the host trees more vulnerable to intense droughts, which are expected to increase due to climate change. We use multispectral (MS) and LiDAR UAV-derived data to determine *Viscum album* ssp. *austriacum* infestation levels at individual tree level in Scots pine (*Pinus sylvestris* L.) forests. First, spectral and structural differences between four infestation levels were assessed employing Kruskal-Wallis test and post hoc Dunn's test for individual tree crowns. Second, machine learning classification algorithms were applied to evaluate infestation levels at the individual tree scale by comparing or combining UAV-derived datasets. Outcomes revealed significant differences between infestation levels in canopy cover and height based on LiDAR derived metrics. Significant changes in vegetation vigor were also found through spectral and textural metrics. Using two vegetation indices (CIRE and NDVI) an overall accuracy of 0.83 was achieved by applying SVM, while combining a spectral metric (NDRE) and a LiDAR metric (D0) resulted in 0.82 accuracy with SVM. Using only LiDAR variables, we obtained an accuracy of 0.64 with SVM and RF. This approach demonstrates their value for detecting and characterizing morphological changes in up to four levels of mistletoe infestation at individual trees in Mediterranean Scots pine forests, lending support to forest management monitoring.

Keywords: UAV; multispectral; LiDAR; machine learning; forest health monitoring; mistletoe.

1. Introduction

Hemiparasitic plants are considered a biotic factor that affects forest ecosystems worldwide, leading to the decline of forest stands (Sangüesa-Barreda et al., 2013; Dobbertin, 2005). In combination with abiotic factors such as prolonged droughts, prone to increase its frequency under current global warming, they are considered as a contributing stress factor for pine vulnerability (Dobbertin & Rigling, 2006; Sangüesa-Barreda et al., 2013; Allen et al., 2010; Sabrina et al., 2020). In fact, ongoing temperature rise and shifts in precipitation patterns make predicting pest dynamics increasingly challenging (Torres et al., 2021). The monitoring and management of hemiparasitic plants is of great interest in southern distribution limits (Zuber, 2004).

Viscum album L. is an evergreen hemiparasitic plant with persistent haustorium that is connected to the host tree through one-way water flow, enabling the transfer of photosynthates and nutrients between the host and the parasite (Glatzel & Geils, 2009; Hernández-Jiménez, 2020). The ssp. *austriacum* is the one found on pines such as *P. sylvestris*, *P. halepensis*, *P. nigra*, and less frequently on *P. pinaster* and *P. uncinata* (Hernández-Alonso et al., 2001; Zuber, 2004). The presence of mistletoe is common and necessary, as its fruits provide food for birds and its leaves serve as sustenance for insects (Mathiasen et al., 2008). The distribution area of *V. album* ranges from 10º W to 80º E, and from 60º N to 35º S, with the Mediterranean Sea marking the southern boundary and the Atlantic Ocean the western boundary (Zuber, 2004). It appears in areas below 1000 meters in altitude, but when exposed to sunlight, it can be found at higher elevations (Zuber, 2004). The presence of mistletoe decreases the vigor and growth of the host and may also exacerbate its water stress during periods of drought (Sangüesa-Barreda et al., 2018). Under water deficit situations, if prolonged over time, can lead to the depletion of the tree's resources and begin to show symptoms of decline or complete death (Sancho-Knapik et al., 2017) as seen in Mediterranean Scots pine forests within the Iberian System.

The abundance of mistletoe in tree canopies is generally assessed through *in situ* studies, which involve high human costs. Though, determining the degree of infestation by fieldwork is challenging because mistletoe typically grows in the upper canopy. The integration of remote sensing data, captured at zenith position, offers quantitative insights to complement in situ surveys enabling spatially detailed monitoring. Remote sensing is a highly promising data source for monitoring forest health and is continuously evolving (Tymińska-Czabańska et al., 2024; Senf et al., 2018). This method can offer an automated and customized solution for accurately detecting and classifying mistletoe (Sabrina et al., 2020). Mistletoe research has been conducted using data collected from multispectral imagery from satellite as done by Thapa (2013), unmanned aerial vehicle (UAV) at ~30 m with hyperspectral sensor, as used by Ančić et al. (2014), and hyperspectral bands and LiDAR data from airborne flights as applied by Barbosa et al. (2016). The combination of high spatial and temporal resolutions, adaptability, and reduced operational expenses makes UAVs a viable substitute to traditional remote sensing platforms (Guimarães et al., 2020).

UAVs are rapidly advancing as an innovative technology for monitoring forest ecosystem health (Torres et al., 2021). Ecke et al. 2022 review their application for this purpose, while Missarov et al. (2024) focus on the use of both UAVs and manned aircraft in mistletoe research. Tymińska-Czabańska et al. (2024) aim to assess the probability of mistletoe presence in *Pinus sylvestris* L. stands using UAV and ALS. Maes et al. (2018) analyze interactions between host and mistletoe by UAV-based infrared thermography. Miraki et al. (2021) used RGB data from UAVs (collected during winter and summer flights in mixed broadleaved forests) to derive a CHM, subsequently used to segment individual trees and classify them as infested and non-infested using RGB bands and Random Forest. León-Bañuelos et al. (2020) use RGB UAV-derived data to identify phenological stages of *Arceuthobium globosum* using colorimetric ranges at pixel level (CRPL) algorithm. Miszczyszyn & Wezyk (2022) investigate the suitability of high-resolution RGB and multispectral data from UAVs, along with derived vegetation indices, for monitoring mistletoe in pine stands. They outline a method utilizing machine learning algorithms like SVM and RF, which could significantly advance mistletoe research. Therefore, multispectral data have been used to mistletoe identification. Mejia-Zuluaga et al. (2022) present a Genetic Programming (GP) method for the automated design of a model utilizing multispectral UAV images to identify mistletoe. On the other hand, Missarov et al. (2022) propose a drone LiDAR for mistletoe recognition and monitoring, a technology also employed by Barbosa et al. (2016). These authors used LiDAR to determine the average height of infested trees, the relative height of mistletoe in the tree canopies, combined with fieldwork, and to classify the landscape structure, which helped identify areas where mistletoe is most prevalent. Thapa (2013) used LiDAR to derive a CHM, which was employed to determine the center of the plot and map the individual tree locations within it.

In this study, we determine the *Viscum album* ssp. *austriacum* infestation levels at individual tree scale on Scots pine forests by using multispectral and LiDAR UAV-derived data. Our aims are (i) to identify the existence of spectral and structural differences between up to four mistletoe infestation levels and (ii) evaluate the potential of multispectral and LiDAR UAV-derived metrics to classify infestation levels, comparing and combining LiDAR and multispectral UAV-derived datasets.

2. Material and methods

2.1 Study area and field data collection

The study area is located in Sierra de Gúdar, within the Iberian Range in Teruel region province (Aragón, Spain). The area covers 20 hectares, corresponding to UAV flights equipped with RGB, multispectral and LiDAR sensors within a public-use forest stand. The stand is dominated by Scots pine (*Pinus sylvestris* L.), which constitutes the southern limit of the species' distribution in the western mediterranean and accompanied by *Juniperus* ssp. The area ranges in elevation from 1600 to 1800 m a.s.l., and the mean annual temperature is 9.4ºC and annual rainfall averages 700 mm. The main lithology is composed of Early Cretaceous marls and marls limestones.

Field data collection was carried out in 55 selected trees (Figure 1). For each tree, a mistletoe infection level (from 1 to 4) was assigned in the field based on expert knowledge. The established levels were determined using a three pair wise including researchers and forest health experts from the Aragon Forest Service.

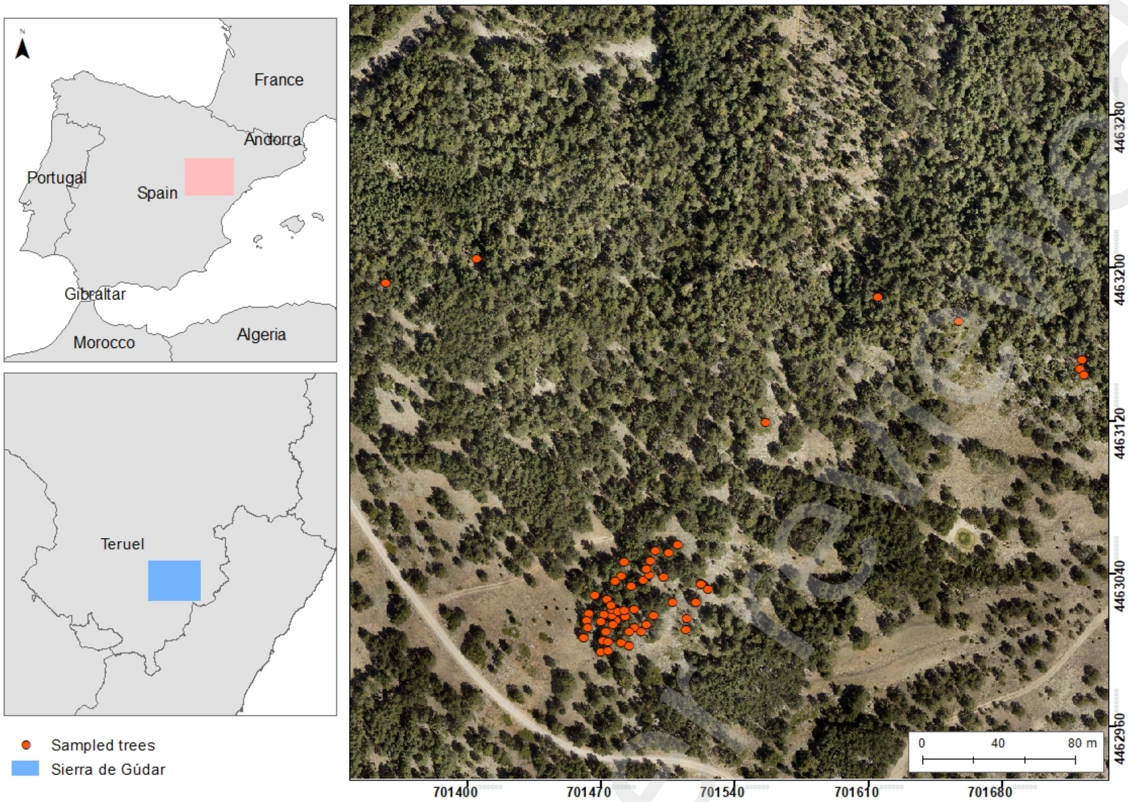

Figure 1. Location of the research area and spatial distribution of the 55 sampled trees within the 30T HUSE grid of the UTM coordinate system. The orthomosaic was obtained from imagery captured during a DJI Matrice 300 RTK drone flight using an RGB sensor conducted in April 2023.

The established levels of mistletoe infection in Scots pine were as follows: Level 1, no presence of mistletoe or only one clump. Level 2, more than one mistletoe clump but green needle foliage is more abundant than mistletoe. Level 3, green needle foliage is less abundant than mistletoe. Level 4, a tree with abundant mistletoe without green needle foliage or one that is dead. These levels were determined according to infestation criteria established by the Aragón Region Forest Health Monitoring Network (Gobierno de Aragón et al., 2020). The first field campaign was conducted in July 2023, involving a minor sampling based on UAV, followed by a second campaign in May 2024 to re-evaluate the infestation levels. The trees analyzed were selected based on the existence of no changes in mistletoe infestation levels and defoliation between UAV data acquisition in 2023 respect to the re-evaluation field campaign in 2024.

2.2 UAV multispectral and LiDAR data capture and processing

Data collection involved two flight missions using a DJI Matrice 300 platform. The drone platform was fitted with Global Navigation Satellite System (GNSS) and real-time Kinematic (RTK) weighting 6.3 kg. The flights were conducted in April 11, 2023.

The first flight utilized the Micasense Altum P camera to acquire multispectral imagery across RGB and near infrared wavelengths. The camera weighs 577 g and has dimensions of 11.0 x 8.0 x 6.9 cm. The flight altitude was set at 70 m, with a 20 m swath width, and a speed of 5 m/s was set. The ground sample distance (GSD) was 3 cm, and a field of view of 50° HFOV x 38° VFOV. The spectral bands were: blue (475 nm), green (560 nm), red (668 nm), red edge (717 nm), and NIR (842 nm).

The second flight equipped a Phoenix Aerial LiDAR Scout Ultra system with Velodyne sensors to generate a LiDAR point cloud, in addition to capture an RGB image. LiDAR sensor weighs 2.2 kg, and has dimensions of 18.5 x 11.6 x 11.6 cm. It includes an inertial measurement unit for accurate management of flight settings. The scan rate was 600 k points/s, with up to 2 returns per pulse with an average accuracy of 55 mm RMSE in z values at a 50 m range. The average survey altitude was set to 85 m and the average approximate survey flight speed was 8.02 m/s.

The trajectory information was managed using PhoenixLiDAR System's Navlab to improve system position and altitude. A precise post-processed trajectory was produced through the combined integration of GNSS and IMU data captured by the LiDAR system. The point cloud was derived in ETRS89 / UTM zone 30N (EPSG:25830) coordinate system and categorized into ground, non-ground, and noise. Subsequently, a digital elevation model (DEM), a digital surface model (DSM), and a canopy height model (CHM) were computed.

The CHM was computed from the difference between the DEM and DSM at 3 cm resolution. The DEM raster was obtained by selecting the ground points to determine the ground level height above sea level. The DSM raster was created considering both vegetation and ground points. The DEM and DSM were created using the LAS Dataset to Raster tool in ArcMap version 10.7.1. The output raster's cell values were defined through a binning approach, with an average assignment to each pixel and linear interpolation for gap filling.

2.3 Individual tree crown delineation

Tree crown delineation was carried out manually. For the digitalization of 55 tree crowns, the true color RGB and false color (NIR-green-blue) multispectral orthomosaics were used, supported by the CHM calculated using the LiDAR data. This approach enabled precise identification of individual tree crowns, facilitating the subsequent analysis of multispectral and LiDAR metrics to study the presence of mistletoe within the canopy. This digitalization has been the basis for the computation of multispectral and LiDAR metrics for each individual tree. The manual delineation was accomplished using ArcMap software version 10.7.1.

2.4. Metrics computation for individual trees

The multispectral information was used to derive vegetation indices and textural features. Concretely, we computed sixteen vegetation indices at 3 cm resolution (see table 1). The use of this dataset of vegetation indices stems from the need to identify those that are most useful for the case study. They are key indicators used to assess health of plants (Thapa, 2013).

Table 1. Vegetation index calculated from spectral bands

Vegetation indices	Formula
NDVI (Normalized Difference Vegetation Index)	NDVI $= \frac{NIR - RED}{NIR + RED}$
GCI (Green Chlorophyll Index)	GCI $= \frac{NIR}{GREEN}$ - 1
CIRE (Chlorophyll Index Red Edge)	CIRE $= \frac{NIR}{RE}$ - 1
NDRE (Normalized Difference Red Edge)	NDRE $= \frac{NIR - RE}{NIR + RE}$
ETA (η)	$\eta = \frac{2\,(NIR\text{^}2 - RED\text{^}2) + 1.5NIR + 0.5RED}{NIR + RED + 0.5}$
GEMI (Global Environmental Monitoring Index)	GEMI $= \eta\,(1 - 0.25\eta) - \frac{RED - 0.125}{1 - RED}$
GNDVI (Green Normalized Difference Vegetation Index):	GNDVI $= \frac{NIR - GREEN}{NIR + GREEN}$
CVI (Chlorophyll Vegetation Index):	CVI $= \frac{NIR \times RED}{GREEN\text{^}2}$
SAVI (Soil-Adjusted Vegetation Index):	SAVI $= \frac{(1 + L)(NIR - RED)}{NIR + RED + L}$
MCARI (Modified Chlorophyll Absorption Ratio Index):	MCARI $= (\frac{RED - RE}{RE - GREEN}) \times NIR$
MSI (Moisture Stress Index):	MSI $= \frac{NIR}{RED}$
RI (Redness Index):	RI $= \frac{RED\text{^}2}{NIR \times BLUE}$
LCI (Leaf Chlorophyll Index):	LCI $= \frac{NIR - RE}{NIR + RED}$

CCCI (Canopy Chlorophyll Content Index):	CCCI $= (\frac{NIR - RE}{NIR + RE}) / (\frac{NIR - RED}{NIR + RED})$
RDVI (Renormalized Difference Vegetation Index):	RDVI $= \frac{RED}{\sqrt{NIR + RED}}$
SQRT_SR (Square Root of Simple Ratio):	SQRT_SR $= \sqrt{\frac{NIR}{RED}}$

The gray-level co-occurrence matrix (GLCM) was used to calculate textural features for each multispectral band. Particularly, the contrast, homogeneity, dissimilarity, entropy, second moment, mean, variance, correlation, and sum of averages features were selected summing up a total of 45 metrics. Once the vegetation indices and textures were computed, we derived the average value for each metric within the extent of the selected tree crowns for subsequent individual analysis. Metric computation and processing were carried out using the "glcm" and "raster" packages for R environment.

The extent of the digitized individual trees was used to clip the LiDAR-generated 3D data, which was then normalized using LAStools to determine the height above ground level. A set of structural metrics from the normalize LiDAR point clouds was derived related to canopy height, height variability, and canopy density as described by Domingo et al., (2024). A cutoff value of 3 m was applied to filter out ground and understory laser returns before calculating the LiDAR metrics. The metrics were computed using FUSION LDV v.4.50(McGaughey, 2023), lidRmetrics (Tompalski et al., 2024) and lasR (Næsset, 2004) in R environment.

Overall, a total of 167 variables were computed, which involved 16 spectral indices, 45 textural features, and 106 LiDAR structural metrics. These metrics served as based information for the subsequent classification of infection levels (see 2.5).

2.5. Classification of mistletoe infestation levels

Firstly, we assessed the suitability of multispectral and LiDAR derived metrics for mistletoe infestation levels discrimination. Initial analyses revealed that the data were not normally distributed . Metrics were transformed to logarithmic and square root scales as a feasible alternative to data normalization. Though, the Shapiro-Wilk test revealed that the data distribution remained non-normal (p-value < 0.05). The nonparametric Kruskal-Wallis test was used to identify which derived metrics shows statistically significant differences between mistletoe infestation levels at the individual tree scale. Then, the non-parametric Dunn's post hoc test for multiple comparisons was applied to identify which variables differentiated between pairs of trees with different levels of mistletoe infestation and to determine the specific pairs distinguished by each variable (García-Galar et al., 2023; Hoffrén et al., 2023).While similar to the Kruskal-Wallis test, this method can identify the specific groups that shows statistically significant differences, making it useful for selecting suitable metrics that will be subsequently used for classification.

The performance of Random Forest (RF) and Support Vector Machine (SVM), two nonparametric machine learning classification algorithms, were evaluated for classifying trees according to their level of mistletoe infestation based on selected multispectral and LiDAR metrics. We tested various combinations of metrics for the models, including only multispectral data; only LiDAR data; or a combination of both datasets.

SVM was executed utilizing a radial kernel and parameterized with a cost of 200 and a gamma of 0.02. RF was tuned by implementing between 1,000 and 3,000 trees (ntrees) and between 1 and 2 variables in each node (mtry) according to Rodrigues and De la Riva (2014) and García-Galar et al. (2023), and the bias correction was applied. Models were computed in R using "e1071", "MASS", and "randomForest" packages. The dataset was divided into training and testing groups derived from a randomly selected sample of pixels to conduct the classification. The testing dataset was used to validate the models, executed by employing a 25% stratified random selection to cover the different mistletoe infestation levels. Validation was performed over 30 repetitions to obtain more robust results and mean performance values were calculated. To contrast and establish the best classification model, confusion matrices, user's accuracy, producer's accuracy and overall accuracy were assessed

3. Results

3.1. Selection of LiDAR and Multispectral metrics for mistletoe infestation levels classification.

A total of 88 variables were found to be significant. Table 2 shows a selection of multispectral, LiDAR and textures variables with the highest chi-square values obtained after executing Kruskal-Wallis test.

Table 2. Results of the Kruskal-Wallis test.

Type	Metrics	Chi Square	*p*-value
Spectral indices	**CIRE**	44.70	***
	NDRE	44.47	***
	NDVI	39.61	***
	NIR mean	16.49	***

LiDAR	zsd	21.47	***
	zvar	21.47	***
	D1	18.69	***
	D0	18.06	***
	Elev L2	14.91	**
	% all returns above 3.00	12.48	**
	D9	8.61	*

*: *p*-value < 0.05; **: *p*-value < 0.01; ***: *p*-value < 0.001.

Vegetation indices CIRE, NDRE and NDVI presented the highest significant differences between mistletoe infestation levels while NIR mean textural metric showed a lower but significant value. *Viscum album* ssp. *austriacum* induces notable modifications in canopy structure, so LiDAR metrics related to canopy height metrics (moment 2 elevation), variability of canopy heights metrics (standard deviation and variation of the height), and canopy density metrics (D0, D1, D9 and percentage of all returns above 3 meters) were also significant.

After analyzing the metrics utilizing the Kruskal-Wallis test, the Dunn's test was applied. The results in table 3 shows the number of metrics that can differentiate each infestation level.

Table 3. Dunn’s test results. Number of variables that can differentiate between infestation levels.

Groups	Number of variables
Level 1 – level 2	1
Level 1 – level 3	30
Level 1 – Level 4	69
Level 2 – level 3	0
Level 2 – level 4	17
Level 3 – level 4	20

Table 4. Dunn’s test results.

Variables	1-2	1-3	1-4	2-3	2-4	3-4
CIRE	0.8199 (NS)	0.0050 **	5.12E-10 ***	0.6725	0.0010 **	0.3294 (NS)
NDRE	0.8458 (NS)	0.0064 **	5.45E-10 ***	0.7344	0.0010 **	0.2868 (NS)
NDVI	1 (NS)	0.0392	6.05E-09 ***	1 (NS)	0.0009 ***	0.1563 (NS)
zsd	0.2923 (NS)	0.0044 **	0.0001 ***	1 (NS)	0.8502 (NS)	1 (NS)
zvar	0.2923 (NS)	0.0044 **	0.0001 ***	1 (NS)	0.8502 (NS)	1 (NS)

D1	1 (NS)	1 (NS)	0.0004 ***	1 (NS)	0.0650(NS)	0.0158 *
D0	1 (NS)	1 (NS)	0.0007 ***	1 (NS)	0.0394 *	0.0158 *
NIR mean	1 (NS)	1 (NS)	0.0035 *	1 (NS)	0.1819 (NS)	0.0048 *
Elev L2	0.5927 (NS)	0.0024 **	0.0287 *	0.6335 (NS)	1 (NS)	1 (NS)
% all returns above 3.00	1 (NS)	1 (NS)	0.0059 **	1 (NS)	0.1597 (NS)	0.1280 (NS)
D9	1 (NS)	1 (NS)	0.0373 *	1 (NS)	0.2646 (NS)	0.5458 (NS)

*: *p*-value < 0.05; **: *p*-value < 0.01; ***: *p*-value < 0.001; NS: non-significant.

Overall, 13 vegetation indices were able to discern between 3 pairs of mistletoe infestation levels. Additionally, a LiDAR-derived variable, D0, was also able to discern 3 pairs. A total of 26 metrics were able to discern between 2 pairs. These include LiDAR-based variables associated with the variability of canopy heights, the distribution of canopy heights, and canopy density, such standard deviation of elevation values, variation of elevation values, 1st percentile representing the value below which 1% of the data is found, and interquartile distance, respectively. Included in these are metrics derived from multispectral bands, such as the vegetation indices ETA, GEMI, and CCCI, as well as those related to textures of the NIR and blue bands.

Figure 2 presents the selected variables that demonstrate statistically significant differences in Dunn's test between mistletoe infestation levels. The greatest differences were found between infestation Level 1 respect to Level 4

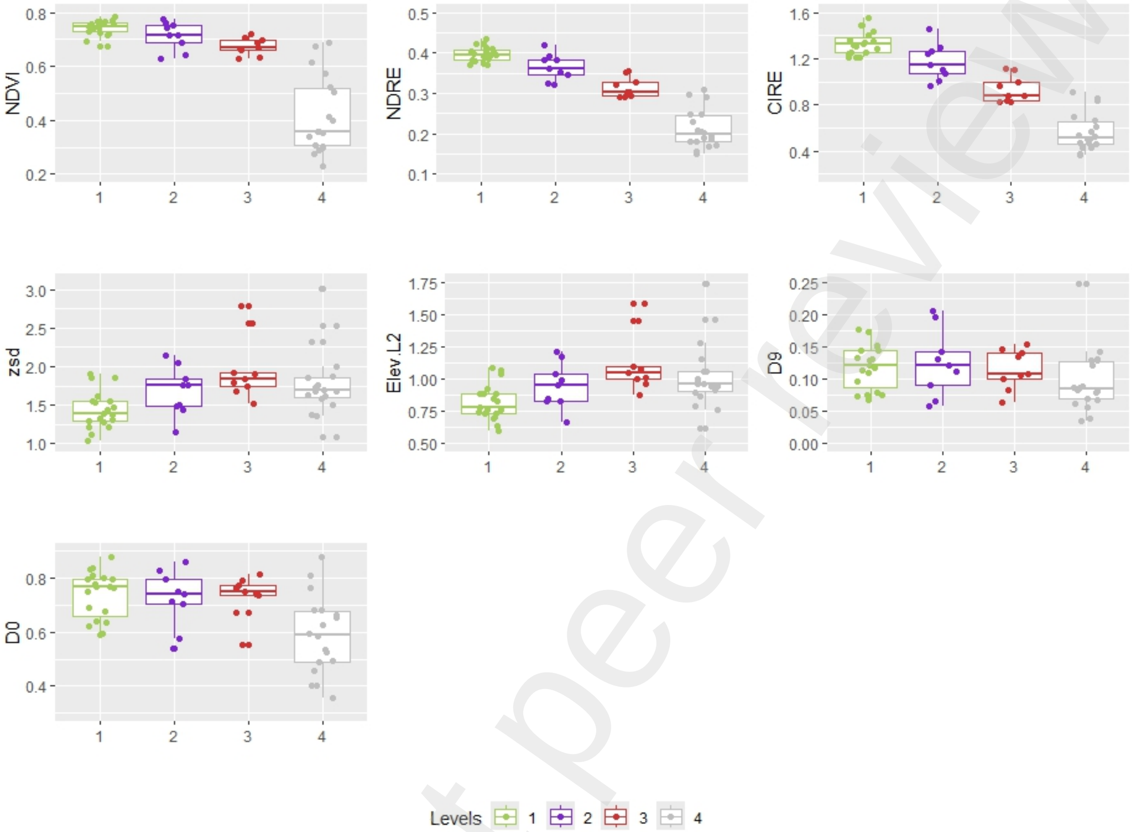

Figure 2. Variables with statistically significant differences in Dunn's test between mistletoe infestation levels.

3.2 Classification of Mistletoe infestation levels classification models.

Mistletoe affects spectral response and structure of the canopy. Vegetation indices were the most important variables for infested trees classification using radial kernel in the SVM algorithm. Using two vegetation indices (CIRE and NDVI) an overall accuracy of 0.83 was achieved by applying SVM, while combining a spectral metric (NDRE) and a LiDAR metric (D0) resulted in 0.82 accuracy with SVM. Using only LiDAR variables, we obtained an accuracy of 0.64 with SVM and RF. Table A1 lists the selected metrics from various groups and sensors, and table 5 presents the results metrics combinations and classification methods.

Table 5. Support Vector Machine (SVM) and Random Forest (RF) Classification methods.

Types of metrics	Metrics	Methods	Fitting phase	Validation
Spectral indices	CIRE+NDVI	SVM	0.823	0.833
	CIRE+NDVI	RF	1	0.733
Spectral indices + LiDAR	NDRE + D0	SVM	0.817	0.817
	NDVI + Elev.L2	RF	1	0.743
LiDAR	zsd + % all ret. above 3.00+ D9	SVM	0.753	0.643
	zsd + D0 + D9	RF	1	0.645

The parameters chosen for the SVM were cost = 200, gamma = 0.02 and a radial basis function kernel. For RF, ntrees = 2000, mtry = 1 with bias correction. Using spectral metrics results in a 15.28% improvement for SVM compared to RF. LiDAR metrics show no difference in performance between the two algorithms. Combining both LiDAR and multispectral metrics, leads to a 9.46% improvement for SVM compared to RF.

Overall, the models shown in Tables 6 to 8, which incorporate spectral, LiDAR, and combined spectral and LiDAR data, exhibited lower accuracy at levels 2 and 3. Errors between close infection levels were to be expected. The boxplots in Figure 2 show the metric similarities, especially between infestation levels 1, 2, and 3.

Table 6. Confusion matrix of the best SVM model with spectral indices metrics.

CIRE+NDVI	Level 1	Level 2	Level 3	Level 4	User's accuracy
Level 1	**19**	4	0	0	82.61%
Level 2	0	**4**	2	0	66.67%
Level 3	0	1	**7**	3	63.64%
Level 4	0	0	0	**15**	100.00%
Prod.'s accuracy	100.00%	44.44%	77.78%	83.33%	

Table 7. Confusion matrix of the best SVM model with LiDAR metrics.

zsd+% all ret. above 3.00+ D9	Level 1	Level 2	Level 3	Level 4	User's accuracy
Level 1	**17**	3	0	2	77.27%
Level 2	0	**5**	2	2	55.56%
Level 3	2	0	**6**	1	66.67%

Level 4	0	1	1	**13**	86.67%
Prod.'s accuracy	89.47%	55.56%	66.67%	72.22%	

Table 8. Confusion matrix of the best SVM model with spectral indices + LiDAR metrics

NDRE + D0	Level 1	Level 2	Level 3	Level 4	User's accuracy
Level 1	**19**	4	0	0	82.61%
Level 2	0	**5**	3	0	62.50%
Level 3	0	0	**6**	2	75.00%
Level 4	0	0	0	**16**	100.00%
Prod.'s accuracy	100%	55.56%	66.67%	88.89%	

The three classification models (Tables 6 to 8) show greater confusion when classifying trees with infestation levels 2 and 3. The producer's accuracy for level 2 ranges from 44% to 55%, while for level 3 it ranges from 66% to 78%. In contrast, level 1 shows an accuracy of 90% to 100%, and level 4 ranges from 72% to 89%. The user's accuracy exceeds 80% in all three models at level 1, ranges from 62% to 66% at level 2, from 63% to 75% at level 3, and from 86% to 100% at level 4.

4. Discussion

The effect of mistletoe in pine forests leads to changes in crown vigor and canopy structure. Mistletoe host experiences a reduction in its water and nutritional supply, causing a progressive atrophy that develops from the implantation site (Hernández-Alonso et al., 2001). This can lead to crown transparency, dead branches, and needle discoloration (Dobbertin, 2005), potentially causing changes in the spectral response and structure of the canopies. Mistletoe infestations lead to reductions in chlorophyll index red edge (CIRE), with a 57.9% decrease between infestation level 1 and level 4, and a 30.1% decrease between level 1 and level 3. The standard deviation of the LiDAR point clouds of trees at level 3 is 37.76% higher compared to the standard deviation at level 1.

Traditional control methods for mistletoe have been costly, highlighting the need for more efficient alternatives for monitoring infestations in Mediterranean pine forests. Standard field methods have limitations, and it is necessary to call for new approaches to assess tree health based on remote sensing, concretely related to mistletoe affection (Ančić et al., 2014). Our study offers a new perspective for forest monitoring by examining individual trees and differentiating infestation levels at an individual scale. Damage severity classification is more relevant for decision-making than mere damage detection, as damage quantification is required in forest pest management (Rullán-Silva et al., 2015). The utilization of UAV platforms opens new ways for analyzing individual tree scales with a three-dimensional perspective on canopy changes (Domingo et al., 2024b).

Spectral and LiDAR UAV derived data, complemented by field sampling, enable the discrimination of infestation levels. Statistically significance differences are identified, and the presence of mistletoe resulted in modifications to canopy morphology and spectral crown response. NDRE, CIRE and NDVI are the most important and significant metrics. The spectral response of infested and non-infested trees differs, particularly across four levels of mistletoe infestation. Spectral signatures reveal insights into the state and structure of both leaves and canopy (Huete, 2012). Damage to host trees causes defoliation and reduced growth (Galiano et al., 2010) eventually leading to tree dead (Reid et al., 1994). Significant reductions in CIRE, NDRE, and NDVI vegetation indices values are observed in the upper canopy due to mistletoe infestation. These variables consider the red, red-edge, and NIR bands. RGB and multispectral UAV data were used by Mejia-Zuluaga et al. (2022), Miszczyszyn & Wezyk (2022), León-Bañuelos et al. (2020), and Miraki et al. (2021) to detect different mistletoes species using visible and NIR bands or vegetation indices. Maes et al. (2018) employed UAV based infrared thermography, showing that the surface temperature of the eucalypt foliage of infested trees was notably higher. Our study also introduces key metrics derived from UAV LiDAR, a data source previously employed by researchers such as Barbosa et al. (2016). However, we leverage LiDAR metrics to distinguish between different levels of infestation, marking a novel application of this technology. Height variability, height distribution and canopy cover density have been the metrics used in classification models. Differences in infestation levels are associated with a more variable and heterogeneous canopy.

The categorization into four levels of mistletoe infection allows us to see which classes are difficult to differentiate. Significant differences are observed between level 1 and level 4, and the most notable confusions occur between the intermediate levels, as shown confusion matrices. This aspect could be explained by the similarity in the structure of trees with similar levels of infestation. LiDAR information is very useful in this context, providing a three-dimensional perspective of pine trees infested by mistletoe. Tree-level metrics, such as canopy heights, variability, and density capture morphological transformations across different infestation degrees. Multispectral data indicate tree health and mistletoe presence in the upper canopy, with spectral responses varying according to infestation severity. Other forest pests, such as the pine processionary moth, have been shown to alter canopy cover and to cause reductions in the upper canopy, as reported by Domingo et al. (2024) using leaf area index (LAI) and mean leaf area density metrics derived from LiDAR.

Miraki et al. (2021) achieve reliable performance using RF to differentiate between two categories (infested and non-infested trees) with both manual and automatic crown segmentation of photogrammetry-derived data in leaf-on and leafless conditions. The overall accuracy is 0.87 for manual segmentation under leaf-off conditions, and 0.76 for the combined leaf-off and leaf-on situations. Barbosa et al. (2016) demonstrate good performance using SVM with a radial function kernel, based on consistent spectral. This approach achieves an accuracy of 86% in classifying two classes: presence and absence of mistletoe. Barbosa et al., using LiDAR data, found that the landscape structure influences the presence of mistletoe, with isolated host trees exhibit twice the infestation load compared to those at the core of forest fragments. In our research we use SVM and RF algorithms to distinguish four infestation levels. When using spectral metrics with SVM (OA = 0.83), although the combination of both sensors also demonstrates significant accuracy (OA = 0.82). RF is not as accurate as SVM in this case, although it achieves optimal results for classifying infestation levels using spectral metrics (OA = 0.73) and by combining spectral and LiDAR data (OA = 0.74). Using only three LiDAR metrics, both algorithms achieved the same accuracy (0.64).

Our study demonstrates the potential of MS and LiDAR UAV data in delineating structural and spectral differences in the crowns infested from *Viscum album* ssp. *austriacum* within a Mediterranean forest dominated by Scots pine. Statistical differences are identified through Kruskal-Wallis and Dunn's test also identified significant differences. These variables are susceptible to morphological and spectral changes in the crowns of host trees according to four infestation levels. His methodology could be applied in future research to wilder areas by developing statistical models to improve forest management. Our outcomes provide insights for similar applications by presenting relevant MS and LiDAR metrics that can be developed into prediction models for other areas. According to Maes et al. (2018) thermal imagery could enable the analysis between infested and non-infested mistletoe trees. Another potential line of research could be to further develop the work initiated by Barbosa et al. (2016) focusing on the landscape characterization in forest stands infested by this hemiparasitic plant, distinguishing between isolated trees, forest edge and forest interior. Combining remote sensing technologies, both active and passive, would be a particularly valuable approach. Satellite imagery could offer the advantage of covering large areas, facilitating the identification of infestation patterns at a regional scale. By integrating these satellite images with UAV data, which provides detailed information on canopy structure and spectral response using multispectral and LiDAR sensors, detection, monitoring, and management strategies for mistletoe in forest ecosystems are significantly enhanced. This combination of tools would enable a more comprehensive and accurate understanding of mistletoe infestation, optimizing its management and control.

5. Conclusion

This research evaluated the potential of combining UAV-derived multispectral imagery and LiDAR point cloud to determine *Viscum album* ssp. *austriacum* affection levels. Our approach demonstrates their value for detecting and characterizing vegetation vigor and morphological changes in up to four levels of mistletoe infestation in Mediterranean Scots pine forest. The most accurate mistletoe infestation classification model was developed using the radial kernel SVM, incorporating two spectral variables: CIRE, and NDVI. The model classification obtained an overall accuracy of 0.83 after validation. LiDAR point cloud derived metrics with RF model achieved a global accuracy of 0.64, which included: standard deviation of elevation values, D0 and D9. Combining both sensor active and passive, classification model with SVM radial kernel achieved an overall accuracy of 0.82, with NDRE and D0. UAV data supports the monitoring of forest management regarding a hemiparasitic plant that currently threatens Mediterranean forests in a context of global change.

Funding

This research was funded by Gobierno de Aragón-Fondo de Inversiones de Teruel (FITE) and Gobierno de España, grant project FITE-2021-DRUIDA and by Gobierno de Aragón research groups S51_23R and S74_23R.

Acknowledgements

We would like to thank the members of the Forest Management Unit-Provincial Service of Teruel for their valuable assistance during the field work.

Appendix A

Table A1. Final metrics included in the models

Group of variables	Variables	Description
Height distribution	Elev.L2	L moment 2 elevation
Height variability	zsd	Standard deviation of elevation values
	zvar	Variation of elevation values
Canopy cover density	D0, D1, D9	% of all returns in 10 equally distributed vertical layers derived by separating the height between the 95th percentile of the height distribution and the 3 m threshold
	% all ret. above 3.00	Percentage of all returns above 3.00
Spectral indices	NDRE	Normalized Difference Red Edge
	CIRE	Index Chlorophyll Index - Red-Edge
	NDVI	Normalized Difference Vegetation Index
Textural features	NIR mean	Mean of the NIR band

Table A2. Number of groups that can differentiate each variable

Variables	**Number of groups**
NDVI, GCI, CIRE, NDRE, GNDVI, CVI, SAVI, MCARI, MSI, RI, LCI, RDVI, SQRT_SR, D0	3
zvar, zsd, zq1, ziqr, zMADmean, zMADmedian, zpcum1, L2, elev.stddev, elev_variance, elev.cv, elev.AAD, elev.MAD.mode, elev.L2, elev.L.CV, Hsd, D1, D2, eta, GEMI, CCCI, NIR_mean, NIR_SA, Blue_ASM, Blue_mean, Blue_SA	2
zmin, zcv, zq5, pzabove2, zentropy, zpcum2, zpcum3, zpcum4, Lcoefvar, lad_max, lad_mean, lad_sum, pz_0.15.2, pz_5.6, pz_8.5.10, Return.2.count, Elev.IQ, Elev.MAD.median, Percentage.first.returns.above.3.00, Percentage.all.returns.above.3.00, Percentage.all.returns.above.mean, Hcv, D3, D4, D5, D6, D7, D8, D9, NIR_homogeneity, NIR_ASM, NIR_entropy, NIR_correlation, RE_homogeneity, RE_ASM, RE_entropy, RE_mean, RE_SA, Red_ASM, Red_mean, Red_correlation, Red_SA, Blue_correlation	1

REFERENCES

Allen, C.D., Macalady, A.K., Chenchouni, H., Bachelet, D., McDowell, N., Vennetier, M., Kitzberger, T., Rigling, A., Breshears, D.D., Hogg, E.H. (Ted), Gonzalez, P., Fensham, R., Zhang, Z., Castro, J., Demidova, N., Lim, J.H., Allard, G., Running, S.W., Semerci, A., Cobb, N., 2010. A global overview of drought and heat-induced tree mortality reveals emerging climate change risks for forests. For. Ecol. Manag. 259, 660–684. https://doi.org/10.1016/j.foreco.2009.09.001

Ančić, M., Pernar, R., Bajić, M., Seletković, A., Koliç, J., 2014. Detecting mistletoe infestation on silver fir using hyperspectral images. IForest 7, 85–91. https://doi.org/10.3832/ifor1035-006

Barbosa, J.M., Sebastián-González, E., Asner, G.P., Knapp, D.E., Anderson, C., Martin, R.E., Dirzo, R., 2016. Hemiparasite–host plant interactions in a fragmented landscape assessed via imaging spectroscopy and LiDAR. Ecol. Appl. 26, 55–66. https://doi.org/10.1890/14-2429

Dobbertin, M., 2006. Pine mistletoe (*Viscum album* ssp. *austriacum*) contributes to Scots pine (*Pinus sylvestris*) mortality in the Rhone valley of Switzerland. For. Pathol. 36, 309–322. https://doi.org/10.1111/J.1439-0329.2006.00457.X

Dobbertin, M., 2005. Tree growth as indicator of tree vitality and of tree reaction to environmental stress: a review. Eur. J. For. Res. 124(4), 319-333. https://doi.org/10.1007/s10342-005-0085-3

Domingo, D., Gómez, C., Mauro, F., Houdas, H., Sangüesa-Barreda, G., Rodríguez-Puerta, F., 2024. Canopy Structural Changes in Black Pine Trees Affected by Pine Processionary Moth Using Drone-Derived Data. Drones, 8(3), 75. https://doi.org/10.3390/drones8030075

Ecke, S., Dempewolf, J., Frey, J., Schwaller, A., Endres, E., Klemmt, H.J., Tiede, D., Seifert, T., 2022. UAV-Based Forest Health Monitoring: A Systematic Review. Remote Sens. 14(13), 3205. https://doi.org/10.3390/rs14133205

Galiano, L., Martínez-Vilalta, J., Lloret, F., 2010. Drought-Induced Multifactor Decline of Scots Pine in the Pyrenees and Potential Vegetation Change by the Expansion of Co-occurring Oak Species. Ecosystems 13, 978–991. https://doi.org/10.1007/s10021-010-9368-8

García-Galar, A., Lamelas, M.T., Domingo, D., 2023. Assessment of Oak Groves Conservation Statuses in Natura 2000 Sacs with Single Photon Lidar and Sentinel-2 Data. Remote Sens. 15(3), 710. https://doi.org/10.3390/rs15030710

Glatzel, G., Geils, B.W., 2009. Mistletoe ecophysiology: Host-parasite interactions. Botany, 87(1), 10-15. https://doi.org/10.1139/B08-096

Gobierno de Aragón, Departamento de Desarrollo Rural y Sostenibilidad, Dirección General de Gestión Forestal, 2020. Redes de evaluación fitosanitaria en las masas forestales de Aragón. Manual de campo. 25 pp. Gobierno de Aragón.

Guimarães, N., Pádua, L., Marques, P., Silva, N., Peres, E., Sousa, J.J., 2020. Forestry Remote Sensing from Unmanned Aerial Vehicles: A Review Focusing on the Data, Processing and Potentialities. Remote Sens. 2020, 12(6), 1046. https://doi.org/10.3390/RS12061046

Hernández-Alonso, R., Martín Bernal, E., Cañada Martín, J.F., Gil Pelegrín, E., Zorrilla Alcaine, F., Pérez Fortea, V., Delgado Soriano, J., Ibarra Ibañez, N., 2001. El muérdago. Gobierno de Aragón, Dirección General del Medio Natural, Servicio de Estudios, Coordinación y Defensa Contra Incendios Forestales. Available at: https://bibliotecavirtual.aragon.es/i18n/catalogo_imagenes/grupo.cmd?path=3714805 (accessed on 1 December 2024)

Hernández-Jiménez, Á., 2020. Evolución de la afección del muérdago (*Viscum album* subsp. *austriacum*) en pinares de la provincia de Zaragoza. Líneas de actuación. Sección Provincial de Zaragoza, Departamento de Agricultura, Ganadería y Medio Ambiente, Gobierno de Aragón. Available at: https://distritoforestal.es/images/AFECCI%C3%93N_DEL_MU%C3%89RDAGO_EN_LA_PROVINCIA_DE_ZARAGOZA_baja_res.pdf

Hoffrén, R., Lamelas, M.T., de la Riva, J., 2023. UAV-derived photogrammetric point clouds and multispectral indices for fuel estimation in Mediterranean forests. Remote Sens. Appl. 31. https://doi.org/10.1016/j.rsase.2023.100997 (accessed on 1 December 2024)

Huete, A.R., 2012. Vegetation Indices, Remote Sensing and Forest Monitoring. Geogr. Compass 6, 513–532. https://doi.org/10.1111/J.1749-8198.2012.00507.X

León-Bañuelos, L.A., Endara-Agramont, A.R., Gómez-Demetrio, W., Martínez-García, C.G., Gabino Nava-Bernal, E., 2020. Identification of *Arceuthobium globosum* using unmanned aerial vehicle images in a high mountain forest of central Mexico. J. For. Res. 31, 1759–1771. https://doi.org/10.1007/s11676-019-00954-5

Maes, W.H., Huete, A.R., Avino, M., Boer, M.M., Dehaan, R., Pendall, E., Griebel, A., Steppe, K., 2018. Can UAV-based infrared thermography be used to study plant-parasite interactions between mistletoe and Eucalypt trees? Remote Sens. 10(12) 2062. https://doi.org/10.3390/rs10122062

Mathiasen, R.L., Nickrent, D.L., Shaw, D.C., Watson, D.M., 2008. Mistletoes: Pathology, systematics, ecology, and management. Plant Dis. 92(7), 988-1006. https://doi.org/10.1094/PDIS-92-7-0988

Mcgaughey, R.J., 2023. FUSION/LDV: Software for LIDAR Data Analysis and Visualization V.4.21. USDA Forest Service. Washington DC, USA.

Mejia-Zuluaga, P.A., Dozal, L., Valdiviezo-N., J.C., 2022. Genetic Programming Approach for the Detection of Mistletoe Based on UAV Multispectral Imagery in the Conservation Area of Mexico City. Remote Sens. 14(3), 801. https://doi.org/10.3390/rs14030801

Miraki, M., Sohrabi, H., Fatehi, P., Kneubuehler, M., 2021. Detection of mistletoe infected trees using UAV high spatial resolution images. J. Plant Dis. Prot. 128, 1679–1689. https://doi.org/10.1007/s41348-021-00502-6

Missarov, A., Krasylenko, Y., Krůček, M., Slavik, M., Nutfullin, B., Král, K., 2021. Drone LiDAR remote sensing for mistletoe recognition and monitoring. Proceedings of the SilviLaser Conference 2021, 300–302. https://doi.org/10.34726/wim.2016

Missarov, A., Sosnovsky, Y., Rydlo, K., Brovkina, O., Maes, W.H., Král, K., Krůček, M., Krasylenko, Y., 2024. Vertical botany: airborne remote sensing as an emerging tool for mistletoe research. Botany, 102(3), 58–71. https://doi.org/10.1139/cjb-2023-0049

Miszczyszyn, J., Wezyk, P., 2022. Detection of mistletoe (*Viscum album* ssp. *austriacum* L.) in Scots pine stands using the MS and RGB UAV high resolution orthophoto. Poster. Available at: https://www.researchgate.net/figure/Poster_fig1_375592451

Næsset, E., 2004. Practical large-scale forest stand inventory using a small-footprint airborne scanning laser. Scand J. For. Res. 19(2), 164–179. https://doi.org/10.1080/02827580310019257

Reid, N., Yan, Z., Fittler, J., 1994. Impact of mistletoes (*Amyema miquelii*) on host (*Eucalyptus blakelyi* and *Eucalyptus melliodora*) survival and growth in temperate Australia. For. Ecol. Manag. 70(1-3), 55–65. https://doi.org/10.1016/0378-1127(94)90074-4

Rullán-Silva, C., Olthoff, A.E., Pando, V., Pajares, J.A., Delgado, J.A., 2015. Remote monitoring of defoliation by the beech leaf-mining weevil *Rhynchaenus fagi* in northern Spain. For. Ecol. Manag. 347, 200–208. https://doi.org/10.1016/j.foreco.2015.03.005

Sabrina, F., Sohail, S., Thakur, S., Azad, S., Wasimi, S., 2020. Use of Deep Learning Approach on UAV imagery to Detect Mistletoe Infestation. IEEE Region 10 Symposium, TENSYMP 2020., Dhaka, 556–559. https://doi.org/10.1109/TENSYMP50017.2020.9230971

Sancho-Knapik, D., Sanz, M.Á., Peguero-Pina, J.J., Niinemets, Ü., Gil-Pelegrín, E., 2017. Changes of secondary metabolites in *Pinus sylvestris* L. needles under increasing soil water deficit. Ann. For. Sci. 74, 24. https://doi.org/10.1007/s13595-017-0620-7

Sangüesa-Barreda, G., Camarero, J.J., Pironon, S., Gazol, A., Peguero-Pina, J.J., Gil-Pelegrín, E., 2018. Delineating limits: Confronting predicted climatic suitability to field performance in mistletoe populations. J. Ecol. 106, 2218–2229. https://doi.org/10.1111/1365-2745.12968

Sangüesa-Barreda, G., Linares, J.C., Julio Camarero, J., 2013. Drought and mistletoe reduce growth and water-use efficiency of Scots pine. For. Ecol. Manage 296, 64–73. https://doi.org/10.1016/J.FORECO.2013.01.028

Senf, C., Pflugmacher, D., Zhiqiang, Y., Sebald, J., Knorn, J., Neumann, M., Hostert, P., Seidl, R., 2018. Canopy mortality has doubled in Europe's temperate forests over the last three decades. Nat. Commun 9, 4978. https://doi.org/10.1038/s41467-018-07539-6

Thapa, S., 2013. Detection and mapping of incidence of *Viscum album* in *Pinus sylvestris* forest of southern Alpe using satellite and airborne imagery. [Master's thesis]. University of Twente. Available at: http://essay.utwente.nl/84727/1/thapa.pdf

Tompalski, P.; Roussel, J.; Woods, M.; Hambrecht, L. Available at: https://github.com/ptompalski/lidRmetrics (accessed on 3 December 2024).

Torres, P., Rodes-blanco, M., Viana-soto, A., Nieto, H., García, M., 2021. The Role of Remote Sensing for the Assessment and Monitoring of Forest Health: A Systematic Evidence Synthesis. Forests 12, 1134. https://doi.org/10.3390/F12081134

Tymińska-Czabańska, L., Janiec, P., Hawryło, P., Ślopek, J., Zielonka, A., Netzel, P., Janczyk, D., Socha, J., 2024. Modeling the effect of stand and site characteristics on the probability of mistletoe infestation in Scots pine stands using remote sensing data. For. Ecosyst. 11, 100191. https://doi.org/10.1016/J.FECS.2024.100191

Zuber, D., 2004. Biological Flora of Central Europe Biological flora of Central Europe: *Viscum album* L. Flora 199, 181-203. https://doi.org/10.1078/0367-2530-00147

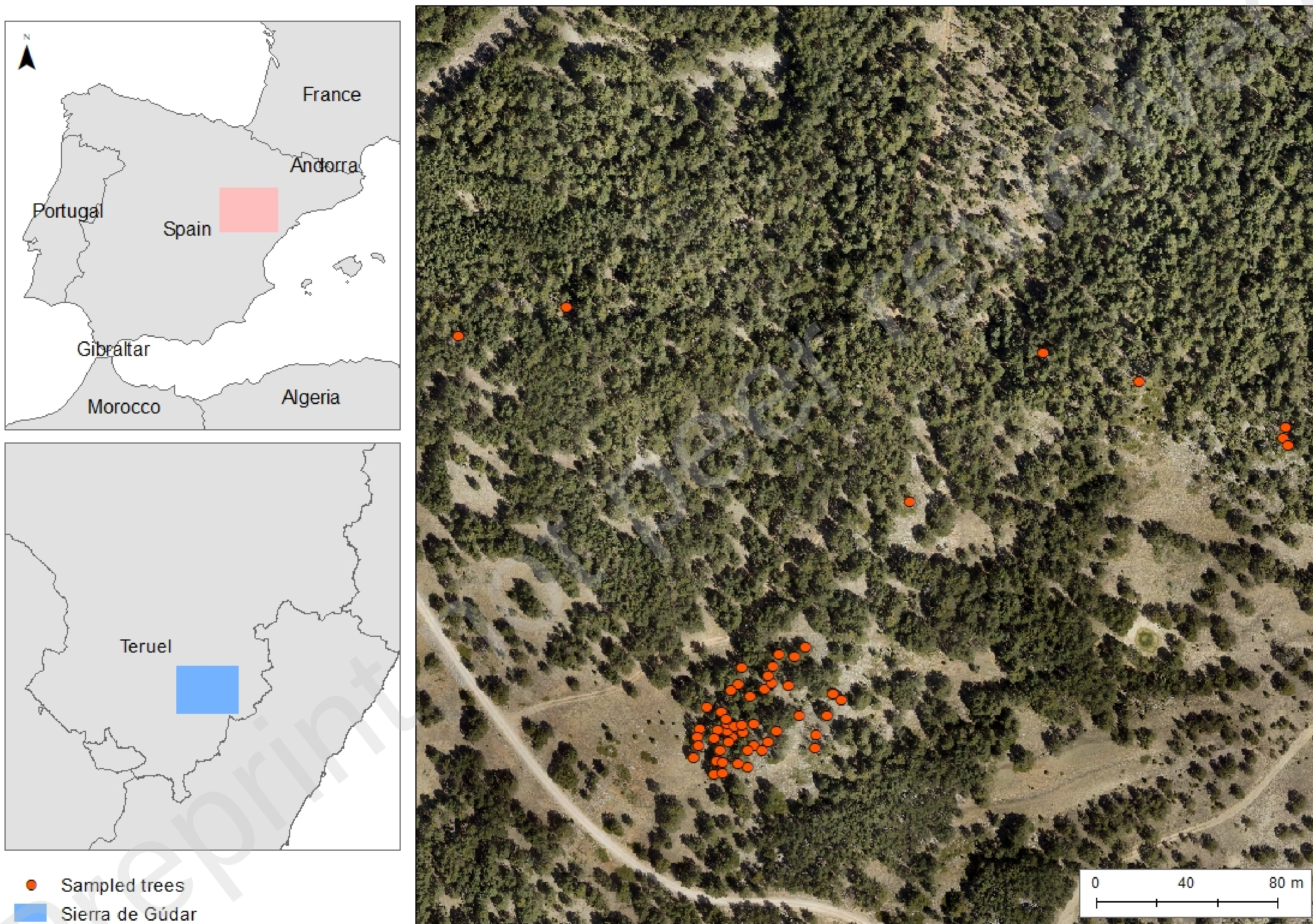

France
Andorra
Portugal
Spain
Gibraltar
Morocco
Algeria
Teruel
Sampled trees
Sierra de Gúdar
0
40
80 m
701400
701470
701540
701610
701680
4463280
4463200
4463120
4463040
4462960

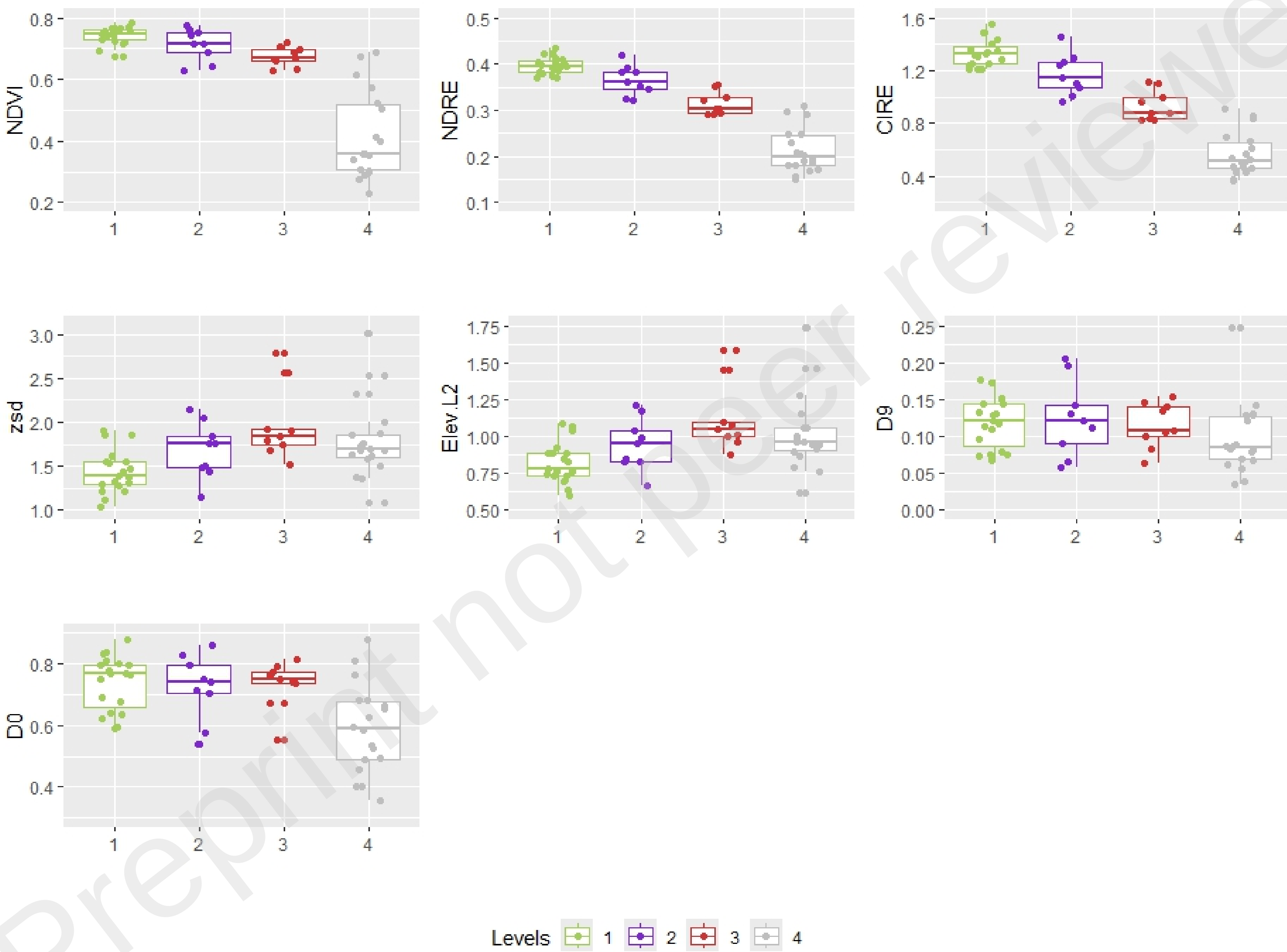
NDVI
NDRE
CIRE
zsd
Elev.L2
D9
D0
Levels
1
2
3
4

Table 1. Vegetation index calculated from spectral bands

Vegetation index	Formula
NDVI (Normalized Difference Vegetation Index)	NDVI $= \frac{NIR - RED}{NIR + RED}$
GCI (Green Chlorophyll Index)	GCI $= \frac{NIR}{GREEN}$ - 1
CIRE (Chlorophyll Index Red Edge)	CIRE $= \frac{NIR}{RE}$ - 1
NDRE (Normalized Difference Red Edge)	NDRE $= \frac{NIR - RE}{NIR + RE}$
ETA (η)	$\eta = \frac{2\,(NIR\text{^}2 - RED\text{^}2) + 1.5NIR + 0.5RED}{NIR + RED + 0.5}$
GEMI (Global Environmental Monitoring Index)	GEMI $= \eta\,(1 - 0.25\eta) - \frac{RED - 0.125}{1 - RED}$
GNDVI (Green Normalized Difference Vegetation Index):	GNDVI $= \frac{NIR - GREEN}{NIR + GREEN}$
CVI (Chlorophyll Vegetation Index):	CVI $= \frac{NIR \times RED}{GREEN\text{^}2}$
SAVI (Soil-Adjusted Vegetation Index):	SAVI $= \frac{(1 + L)(NIR - RED)}{NIR + RED + L}$
MCARI (Modified Chlorophyll Absorption Ratio Index):	MCARI $= (\frac{RED - RE}{RE - GREEN}) \times NIR$
MSI (Moisture Stress Index):	MSI $= \frac{NIR}{RED}$
RI (Redness Index):	RI $= \frac{RED\text{^}2}{NIR \times BLUE}$
LCI (Leaf Chlorophyll Index):	LCI $= \frac{NIR - RE}{NIR + RED}$
CCCI (Canopy Chlorophyll Content Index):	CCCI $= (\frac{NIR - RE}{NIR + RE}) / (\frac{NIR - RED}{NIR + RED})$
RDVI (Renormalized Difference Vegetation Index):	RDVI $= \frac{RED}{\sqrt{NIR + RED}}$
SQRT_SR (Square Root of Simple Ratio):	SQRT_SR = $\sqrt{\frac{NIR}{RED}}$

Table 2. Results of the Kruskal-Wallis test.

Type	Metrics	Chi Square	*p*-value
Spectral indices	**CIRE**	44.70	***
	NDRE	44.47	***
	NDVI	39.61	***
	NIR mean	16.49	***
LiDAR	**zsd**	21.47	***
	zvar	21.47	***
	D1	18.69	***
	D0	18.06	***
	Elev L2	14.91	**
	% all returns above 3.00	12.48	**

	D9	8.61	*

*: *p*-value < 0.05; **: *p*-value < 0.01; ***: *p*-value < 0.001.

Table 3. Dunn's test results. Number of variables that can differentiate between infestation levels.

Groups	Number of variables
Level 1 – level 2	1
Level 1 – level 3	30
Level 1 – Level 4	69
Level 2 – level 3	0
Level 2 – level 4	17
Level 3 – level 4	20

Table 4. Dunn's test results.

Variables	1-2	1-3	1-4	2-3	2-4	3-4
CIRE	0.8199 (NS)	0.0050 **	5.12E-10 ***	0.6725	0.0010 **	0.3294 (NS)
NDRE	0.8458 (NS)	0.0064 **	5.45E-10 ***	0.7344	0.0010 **	0.2868 (NS)
NDVI	1 (NS)	0.0392	6.05E-09 ***	1 (NS)	0.0009 ***	0.1563 (NS)
zsd	0.2923 (NS)	0.0044 **	0.0001 ***	1 (NS)	0.8502 (NS)	1 (NS)
zvar	0.2923 (NS)	0.0044 **	0.0001 ***	1 (NS)	0.8502 (NS)	1 (NS)
D1	1 (NS)	1 (NS)	0.0004 ***	1 (NS)	0.0650(NS)	0.0158 *
D0	1 (NS)	1 (NS)	0.0007 ***	1 (NS)	0.0394 *	0.0158 *
NIR mean	1 (NS)	1 (NS)	0.0035 *	1 (NS)	0.1819 (NS)	0.0048 *
Elev L2	0.5927 (NS)	0.0024 **	0.0287 *	0.6335 (NS)	1 (NS)	1 (NS)
% all returns above 3.00	1 (NS)	1 (NS)	0.0059 **	1 (NS)	0.1597 (NS)	0.1280 (NS)
D9	1 (NS)	1 (NS)	0.0373 *	1 (NS)	0.2646 (NS)	0.5458 (NS)

*: *p*-value < 0.05; **: *p*-value < 0.01; ***: *p*-value < 0.001; NS: non-significant.

Table 5. Support Vector Machine (Svm) and Random Forest (RF) Classification methods.

Types of metrics	Metrics	Method	Fitting phase	Validation
Spectral indices	CIRE+NDVI	SVM	0.823	0.833
	CIRE+NDVI	RF	1	0.733
Spectral indices + LiDAR	NDRE + D0	SVM	0.817	0.817
	NDVI + Elev.L2	RF	1	0.743

LiDAR	zsd + % all ret. above 3.00+ D9	SVM	0.753	0.643
	zsd + D0 + D9	RF	1	0.645

Table 6. Confusion matrix of the best SVM model with spectral indices metrics.

CIRE+NDVI	Level 1	Level 2	Level 3	Level 4	User's accuracy
Level 1	**19**	4	0	0	82.61%
Level 2	0	**4**	2	0	66.67%
Level 3	0	1	**7**	3	63.64%
Level 4	0	0	0	**15**	100.00%
Prod.'s accuracy	100.00%	44.44%	77.78%	83.33%	

Table 7. Confusion matrix of the best SVM model with LiDAR metrics.

zsd+% all ret. above 3.00+ D9	Level 1	Level 2	Level 3	Level 4	User's accuracy
Level 1	**17**	3	0	2	77.27%
Level 2	0	**5**	2	2	55.56%
Level 3	2	0	**6**	1	66.67%
Level 4	0	1	1	**13**	86.67%
Prod.'s accuracy	89.47%	55.56%	66.67%	72.22%	

Table 8. Confusion matrix of the best SVM model with spectral indices + LiDAR metrics

NDRE + D0	Level 1	Level 2	Level 3	Level 4	User's accuracy
Level 1	**19**	4	0	0	82.61%
Level 2	0	**5**	3	0	62.50%
Level 3	0	0	**6**	2	75.00%
Level 4	0	0	0	**16**	100.00%
Prod.'s accuracy	100%	55.56%	66.67%	88.89%	